Myricetin, quercetin and catechin-gallate inhibit glucose uptake in isolated rat adipocytes

Pablo STROBEL*[1], Claudio ALLARD*†, Tomás PEREZ-ACLE†, Rosario CALDERON*, Rebeca ALDUNATE* and Federico LEIGHTON*

*Molecular Nutrition Laboratory, Faculty of Biological Sciences, Universidad Católica de Chile, Casilla 114-D, Santiago, Chile, and †Center for Genomics and Bioinformatics, Faculty of Biological Sciences, Universidad Católica de Chile, Casilla 114-D, Santiago, Chile

The facilitative glucose transporter, GLUT4, mediates insulin-stimulated glucose uptake in adipocytes and muscles, and the participation of GLUT4 in the pathogenesis of various clinical conditions associated with obesity, visceral fat accumulation and insulin resistance has been proposed. Glucose uptake by some members of the GLUT family, mainly GLUT1, is inhibited by flavonoids, the natural polyphenols present in fruits, vegetables and wine. Therefore it is of interest to establish if these polyphenolic compounds present in the diet, known to be effective antioxidants but also endowed with several other biological activities such as protein-tyrosine kinase inhibition, interfere with GLUT4 function. In the present study, we show that three flavonoids, quercetin, myricetin and catechin-gallate, inhibit the uptake of methylglucose by adipocytes over the concentration range of 10–100 μM. These three flavonoids show a competitive pattern of inhibition, with $K_i = 16$, 33.5 and 90 μM respectively. In contrast, neither catechin nor gallic acid inhibit methylglucose uptake. To obtain a better understanding of the interaction among GLUT4 and flavonoids, we have derived a GLUT4 three-dimensional molecular comparative model, using structural co-ordinates from a GLUT3 comparative model and a mechanosensitive ion channel [PDB (Protein Data Bank) code 1MSL] solved by X-ray diffraction. On the whole, the experimental evidence and computer simulation data favour a transport inhibition mechanism in which flavonoids and GLUT4 interact directly, rather than by a mechanism related to protein-tyrosine kinase and insulin signalling inhibition. Furthermore, the results suggest that GLUT transporters are involved in flavonoid incorporation into cells.

Key words: catechin-gallate, flavonoid, glucose transporter, molecular dynamics, myricetin, quercetin.

INTRODUCTION

Glucose enters many cells through the activity of glucose transporters (GLUTs), a family of membrane-spanning proteins [1,2]. GLUT4, the predominant glucose transporter isoform in muscles and adipose tissue, is the major carrier involved in insulin-stimulated glucose transport [3]. Insulin increases glucose uptake in these cells by stimulating GLUT4 translocation to the plasma membrane, from a sequestered site at the intracellular microsomal compartment [4]. Flavonoids are a group of polyphenol compounds present in plant foods and their presence in tea, onions, red wine, berries and some medicinal plants is often highlighted for their health-enhancing properties [5]. The biological effects of flavonoids are commonly attributed to their redox antioxidant properties rather than to other molecular interactions [6]. However, flavonoids were recently reported to be competitive inhibitors of glucose uptake in erythrocytes, U937 cells and HL-60 cells and they also inhibit GLUT-mediated dehydroascorbic acid uptake by HL-60, U937 and Jurkat cells [7]. Genistein, quercetin, myricetin, morin, rhamnetin and isorhamnetin inhibit GLUT1-mediated glucose transport through a direct interaction with this membrane protein [8–10]. In fact, a better understanding of the interaction of flavonoids with the cell membrane and, more importantly, of their uptake is necessary to understand the numerous biological effects of the different classes of flavonoids in various cell types and tissues [11].

Studies of transport of flavonoid have been made in Caco-2 cells and rat small intestine, where flavonoid glycosides are incorporated using SGLT1 (sodium-dependent glucose transporter 1) and monocarboxylate transporter, as described for epicatechin-3-gallate [12]. The multidrug-resistance-associated protein isoforms 2 and 3 have been shown to be an important efflux transporter of flavonoids, mainly the glucuronide and sulphate conjugates [11,12]. However, the effect of these flavonoids on GLUT4-mediated glucose transport in adipocytes in the presence of insulin has not been described; also, the potential of other flavonoids to inhibit insulin-stimulated glucose transport in these cells has not been described. Some flavonoids inhibit protein-tyrosine kinases [13], but this does not exclude a possible direct interaction with the transporter. In fact, the isoflavone genistein does not inhibit the insulin receptor kinase activity, yet it markedly decreases basal and insulin-stimulated glucose uptake in rat adipocytes, without compromising the insulin-induced recruitment of GLUT4 to the plasma membrane [14]. On the basis of the evidence in favour of a direct interaction among flavonoids and glucose transporters, we performed *in vitro* uptake competition studies and we evaluated the molecular dynamics of the interaction among GLUT4 and flavonoids, employing a comparative model of GLUT4. Conserved sequence motifs suggest the existence of shared structural features, confirmed by *in situ* labelling and mutagenesis studies, among glucose transporter proteins GLUTs. Each GLUT protein has 12 membrane-spanning domains, organized to form an aqueous channel. Helices 2, 5, 7, 10 and 11 are related to D-glucose movement across the internal pore. Helix 7 has the residues Gln-Leu-Ser, a motif known as the QLS site, widely conserved in the GLUT transporter family [15].

Initial characterization of the secondary structure of GLUTs by CD and Fourier-transform infrared spectroscopy reveals that

Abbreviations used: 3D, three-dimensional; AQP1, acquaporin 1; IRS1, insulin receptor substrate 1; MscI, mechanosensitive ion channel.

[1] To whom correspondences should be addressed (email pstrobel@bio.puc.cl).

more than 70 % of the protein adopts an α-helical conformation [16]. Because of the complexity of GLUTs, membrane proteins that easily aggregate into dimers and tetramers [17], it is difficult to determine their 3D (three-dimensional) structure by X-ray crystallography or NMR. Molecular modelling can provide important insights into the structure and function of a protein when the high-resolution structure has not been established. This approach relies on structural data from a suitable homologue or template molecule to develop a plausible model [18].

Using a GLUT4 3D molecular model, a molecular dynamics-simulated annealing at the protein pore region was performed with D-glucose, with the flavonoids quercetin and catechin-gallate and with the GLUT4-binding alkaloid cytochalasin B. These computer simulation data revealed discrete conformational changes and direct, non-bonded residue interactions that support inhibition of glucose transport by direct interaction of flavonoids with the GLUT4 transporter.

EXPERIMENTAL

Materials

Quercetin, myricetin, catechin-gallate, gallic acid, catechin, phloretin, cytochalasin B and collagenase Type II were purchased from Sigma (St. Louis, MO, U.S.A.). Insulin was purchased from Lilly France, 3-*O*-[^{3}H]methyl-D-glucose was from NEN Life Science Products, anti-nitrotyrosine monoclonal antibody and anti-IRS1 (insulin receptor substrate 1) polyclonal antibody were from Upstate Biotechnology (Lake Placid, NY, U.S.A.). Goat anti-mouse-horseradish peroxidase antibody and anti-rabbit-horseradish peroxidase antibody were obtained from Santa Cruz Biotechnology (Santa Cruz, CA, U.S.A.).

Isolated adipocytes

Adipocytes were prepared by the collagenase method as described by Rodbell [19] from epididymal fat pads of male Wistar rats weighing 200–250 g. To disperse the cells, the tissue was digested at 37 °C in Krebs–Ringer-Hepes buffer (128 mM NaCl, 10 mM Hepes, 5 mM KCl, 5 mM NaH_2PO_4, 1.5 mM $MgSO_4$ and 1.25 mM $CaCl_2$; pH 7.4) containing 3 % (w/v) BSA, 2 mg/ml collagenase and 2 mM glucose. Isolated cells were then washed and suspended in Krebs–Ringer-Hepes buffer (pH 7.4) at 37 °C, supplemented with 3 % BSA and 2.5 mM pyruvate. Cells were counted at an appropriate dilution, in an improved Neubauer counting chamber.

Glucose uptake assays

The rate of 3-*O*-methyl-D-glucose transport was estimated when the *trans* (internal) concentration was zero, using an established procedure [20]. For uptake inhibition studies, individual flavonoids were added to the Krebs–Ringer-Hepes buffer containing 3-*O*-[^{3}H]methylglucose and unlabelled methylglucose. Briefly, 100 μl of a 50 % cell suspension was pipetted rapidly on to 20 μl of Krebs–Ringer-Hepes buffer containing 2 μCi of 3-*O*-[^{3}H]methyl-D-glucose (specific activity, 86.7 Ci/mmol) and adequate concentrations of unlabelled methylglucose, at 37 °C. When needed, the glucose transport was activated by insulin (1 μM), and the cells were incubated for 30 min at 37 °C. The transport process was stopped by the addition of 200 μl of albumin-free Hepes buffer containing 1 mM phloretin and 10 μM cytochalasin B. The cells were then spun through a 400 μl layer of dinonylphthalate in an Eppendorf centrifuge for 20 s at 9000 ***g***. The separated cells were removed from the top of the oil layer with a pipe cleaner. The trapped radioactivity was measured by liquid-scintillation counting. For zero time measurement, stop buffer was added to the cells before the addition of isotope solution.

Quercetin uptake assays

For uptake-inhibition studies, the inhibitor glucose or cytochalasin B was added to the Hepes buffer containing quercetin. Briefly, 100 μl of a 50 % cell suspension was pipetted rapidly on to 20 μl of Krebs–Ringer-Hepes buffer containing 100 μM quercetin at 37 °C. When needed, insulin (1 μM) was added, and the cells were incubated for 30 min at 37 °C. The transport process was stopped by the addition of 200 μl of albumin-free Hepes buffer with 1 mM phloretin and 10 μM cytochalasin B. The cells were then spun through a 400 μl layer of dinonylphthalate in an Eppendorf centrifuge for 20 s at 9000 ***g***. The separated cells were removed from the top of the oil layer with a pipe cleaner. For zero time measurement, stop buffer was added to the cells before the addition of quercetin solution. After the uptake experiments, the quercetin in the cells was extracted with 300 μl of methanol, and the extracts were analysed by reversed-phase HPLC on a Merck Hitachi 7000 series system with a Supelcosil C-18 column, 3.6 mm × 250 mm, with a model 7450A photodiode array detector and an amperometric detector LC-4C (BAS) set at 0.5 μA and + 1.0 V. The mobile phase consisted of 35 % (v/v) methanol in 5 % (v/v) acetic acid with a flow rate of 1 ml/min [21]. Quercetin peak areas were measured at 370 nm.

Immunoprecipitation

Adipocytes (2×10^6 cells/ml) were preincubated with or without 1 μM insulin for 30 min at 37 °C in Krebs–Ringer-Hepes buffer, containing 1 % BSA. Then, 100 μl of the cell suspension was mixed with 20 μl of the same buffer containing the tested flavonoid. After 30 s, the total incubation mixture was diluted with 200 μl of albumin-free Hepes buffer containing 1 mM phloretin. The cells were lysed at 4 °C in 0.3 ml of lysis buffer containing 50 mM Tris/HCl (pH 7.4), 1 % Nonidet P40, 150 mM NaCl, 1 mM EDTA, 1 mM PMSF, 1 μg/ml aprotinin, 1 μg/ml leupeptin, 1 μg/ml pepstatin, 1 mM Na_3VO_4 and 1 mM NaF. The lysates were clarified by centrifugation at 15000 ***g*** for 10 min. After protein content determination, equal amounts of protein (300 mg) were immunoprecipitated with 4 μg/ml anti-IRS overnight at 4 °C. The immunocomplexes were collected on Protein A–agarose beads, by gently rocking at 4 °C for 2 h. Immunoprecipitates were collected by pulsing for 30 s at 14000 ***g***, washed twice with lysis buffer and heated for 5 min at 95 °C in 4 × SDS/PAGE sample buffer. Proteins were separated by SDS/PAGE by the method of Laemmli [22] using an SDS/12 % (w/v) polyacrylamide gel.

Western blotting

After SDS/PAGE, the protein was transferred on to Immun-Blot PVDF membranes (Bio-Rad), blocked using 3 % (w/v) non-fat dried milk in 10 mM phosphate buffer, 150 mM NaCl (pH 7.4) and 0.05 % Tween 20 for 30 min at room temperature (21–23 °C) and then incubated overnight at 4 °C with the anti-phosphotyrosine antibody (1 μg/ml). Immunoreactive bands were visualized using the ECL® Western blotting method (PerkinElmer Life Sciences, Boston, MA, U.S.A.).

GLUT4 3D molecular comparative modelling

The existence of a GLUT3 3D model, reported in [23], and the high sequence identity (85 % identity, 94 % of positive residues) between this structure and GLUT4 supported its use to obtain

a 3D model for GLUT4. In addition, we used an Mscl (mechanosensitive ion channel) model [PDB (Protein Data Bank) code 1MSL] solved by X-ray diffraction at 3.50 Å (1 Å = 0.1 nm) [24] as an additional template for the smoothing of co-ordinate assignment. To perform the co-ordinate assignment process, we used Modeller from Insight II (Accelrys Inc., San Diego, CA, U.S.A.). Modeller, using energy minima criterion, provided four possible structures. For every available structure, we made energy minimization procedures using the molecular mechanics force field CVFF (consistent valence force field) implemented under Discovery from Insight II (Accelrys Inc.). Using PROCHECK [25] to obtain a Ramachandran accomplishment graph, we determined the amount of misplaced Φ and Ψ angles. For each misplaced angle that was not present in any of the template structures, our model was manually corrected according to secondary-structure consensus pattern, reiterating through energy minimization, as described above, until no further misplaced angles were found. All computer simulations were performed in a Silicon Graphics Origin 200, 4 processors cluster.

Molecular dynamics simulated annealing

To evaluate the docking mode and to simulate possible interactions with GLUT4, we used a ligand battery, which included D-glucose, cytochalasin B, quercetin and catechin-gallate, applying the Docking module of Insight II with CVFF. We set up a spherical interface with a 20 Å radius surrounding Gln-295, where each residue was defined as mobile and a possible site for ligand–receptor interaction. This spherical interface explicitly excludes the amino acids involved in the ATP-binding consensus regions described for GLUTs [26]. The Cell Multipole summation method was used to compute weak interactions (Coulomb + van der Waals) and a dielectric constant of 80, distance-dependant, to simulate implicit charge distribution through water. An exhaustive search for docking conformational co-ordinates was performed using Metropolis with an RMS (root mean square) tolerance value of 1. Every accepted conformation was relaxed by molecular dynamics with a reverse temperature gradient (simulated annealing) starting at 500 K and ending at 300 K, with 500 stages of 100 fs per stage, 50 ps in total. For each final conformation, an energy minimization was performed.

The whole computer simulation was performed on a Silicon Graphics Origin 200, 4 processors NUMA link cluster.

RESULTS

Time course of methylglucose uptake

Methylglucose is a non-metabolizable substrate of the transporters and therefore its intracellular concentration will be determined by the rate of incorporation and the rate of reverse flow. Methylglucose transport in rat adipocytes was determined under low-glucose conditions (0.5 mM), to approach the initial rate of glucose uptake value. The time course for the uptake of labelled methylglucose (2 μCi) and methylglucose (0.5 mM) at 37 °C is shown in Figure 1. In insulin-stimulated cells, the apparent rate of accumulation of methylglucose is several times higher than non-stimulated basal cells. Equilibrium is reached at approx. 60 s for both conditions, and the intracellular concentration remains constant. The uptake of methylglucose at 30 s of incubation, both in cells stimulated by insulin and in cells under basal conditions, was used as an approximation to the initial rates of incorporation.

Effect of flavonoids on methylglucose uptake by rat adipocytes

The effect of flavonoids was studied with two flavonols, myricetin and quercetin, and with the flavanol catechin, as free catechin or as catechin-gallate (Figure 2). Quercetin, myricetin and catechin-gallate show a dose-dependent inhibition of insulin-stimulated methylglucose uptake, whereas catechin and gallic acid, as separated compounds, did not inhibit uptake (Figure 3). For myricetin and quercetin, 50 % inhibition was observed at approx. 10 μM. For catechin-gallate, 50 % inhibition was reached at approx. 50 μM. At higher concentrations of the flavonoids quercetin, myricetin and catechin-gallate, transport of methylglucose into adipocytes stimulated with insulin decreased to almost the same level as that of non-insulin-stimulated cells. At 100 μM flavonoid concentration, the inhibition of insulin-stimulated cells was approx. 80 %, reaching values that did not differ statistically from those observed for non-stimulated cells or cells under basal conditions. To examine whether the inhibitory effect observed with catechin-gallate was specifically due to one of the chemical

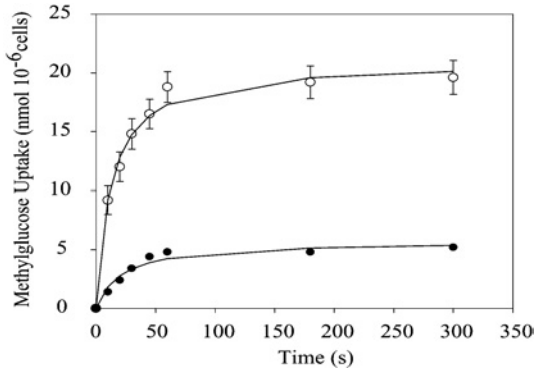

Figure 1 Time course of methylglucose uptake

Cells were incubated for 30 min in the absence (●) or presence (○) of 1 μM insulin before the addition of 2 μCi of 3-*O*-[^{3}H]methyl-D-glucose and 0.5 mM 3-*O*-methyl-D-glucose. Basal values were obtained by preincubating with 1 mM phloretin and 10 μM cytochalasin B, as described in the Experimental section. Values represent the means ± S.D. for four samples. The S.D. values for the data points in the absence of insulin are too small to be seen in the graph.

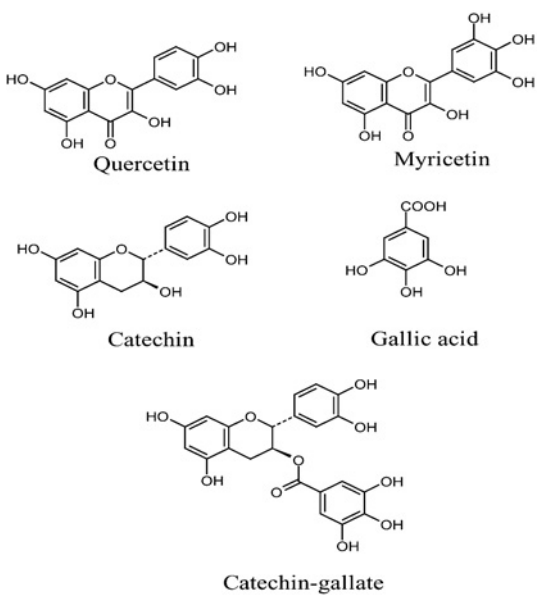

Figure 2 Structure of quercetin, myricetin, catechin, catechin-gallate and gallic acid

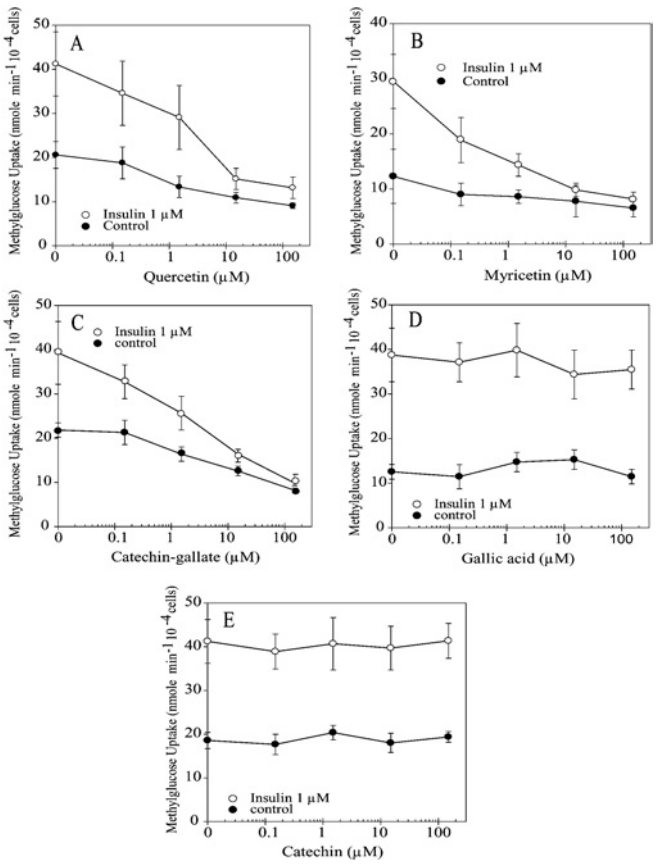

Figure 3 Effect of flavonoids on methylglucose uptake by rat adipocytes

Dose–response curves for (**A**) quercetin, (**B**) myricetin, (**C**) catechin-gallate, (**D**) gallic acid and (**E**) catechin on the transport of methylglucose, measured as uptake in 30 s, in the presence (○) or absence (●) of 1 μM insulin. Results are expressed as percentage of transport in the absence of flavonoids and shown as the means ± S.D. for four samples.

species, catechin or gallic acid, cells under basal conditions and stimulated with insulin were studied at various concentrations of the two compounds. Gallic acid had no effect on methylglucose transport under basal or insulin-stimulated conditions, and catechin did not inhibit insulin-stimulated cells. Therefore activity was detected only with catechin-gallate, the catechin derivative.

Determination of K_i values for quercetin, myricetin and catechin-gallate

To characterize further the pattern of inhibition by flavonoids and to determine the K_i values, inhibition experiments were performed with insulin-stimulated adipocytes. Kinetic analyses of the inhibitory effect on methylglucose transport, observed at different flavonoid concentrations, reveal a competitive pattern of inhibition for quercetin, myricetin and catechin-gallate (Figure 4). The K_i values calculated were 16, 33.5 and 90 μM for quercetin, myricetin and catechin-gallate respectively.

Inhibition of the transport of quercetin

Competition experiments using 30 s transport assays indicated that D-glucose and cytochalasin B inhibit the transport of quercetin into rat adipocytes in the presence of insulin and in control cells. Half-maximal inhibition in the presence of D-glucose and cytochalasin B was observed at approx. 1 mM and 1 μM respectively, in cells preincubated with insulin (Figure 5).

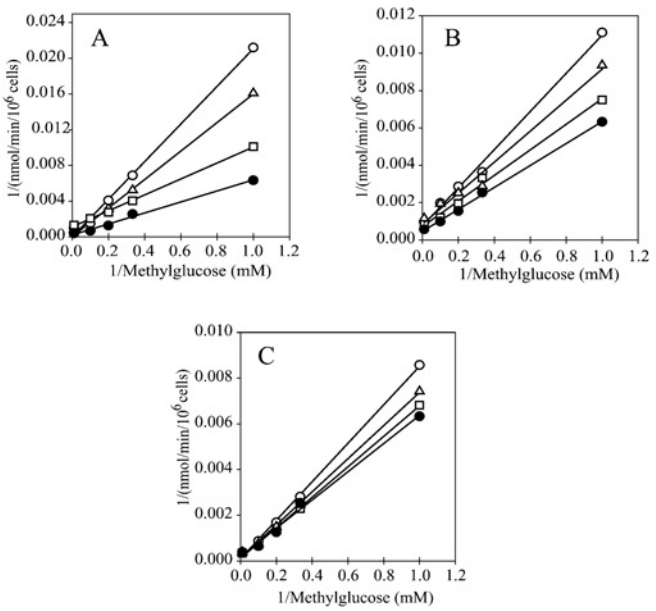

Figure 4 Competitive inhibition by quercetin, myricetin and catechin-gallate of methylglucose uptake into rat adipocytes

Lineweaver–Burk double-reciprocal plots of the effect of flavonoids: (**A**) quercetin, (**B**) myricetin and (**C**) catechin-gallate. Transport of methylglucose at 5, 10, 15, 20 and 40 mM was measured for 30 s in the absence (●) or in the presence of 10 μM (□), 20 μM (△) and 40 μM (○) of flavonoids. Cells were preincubated for 30 min with 1 μM insulin. Secondary plots of the effects of flavonoids on the substrate dependence of methylglucose transport were used to calculate the K_i values. Each experimental value shown corresponds to the mean for four samples.

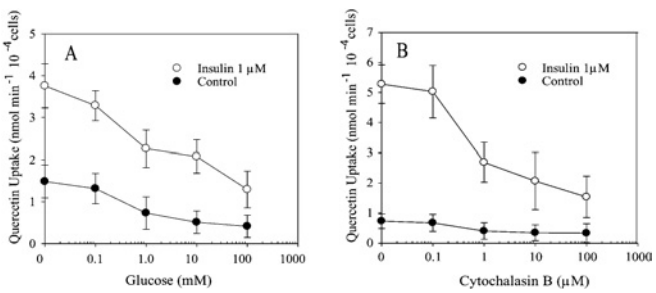

Figure 5 Inhibition of quercetin uptake by rat adipocytes

Semi-exponential plot of the concentration dependence for the inhibition of quercetin transport into rat adipocytes by D-glucose (**A**) and cytochalasin B (**B**), measured as uptake in 30 s in the presence (○) or absence (●) of 1 μM insulin. Results are expressed as percentage of transport in the absence of flavonoids and are shown as means ± S.D. for four samples.

Quercetin does not inhibit protein tyrosine phosphorylation in rat adipocytes

The activity of GLUT4 can be modulated by protein phosphorylation [27] and some flavonoids inhibit insulin receptor tyrosine kinase-catalysed phosphorylation of exogenous substrates [28]. Our results support the hypothesis that the inhibitory effect of quercetin on glucose uptake is the consequence of a direct action on GLUT4, rather than the result of an indirect mechanism involving inhibition of cellular protein-tyrosine kinases. To evaluate the role of flavonoids on protein tyrosine phosphorylation, we studied isolated adipocytes that had been preincubated with insulin (1 μM) and control adipocytes. The adipocytes were immunoprecipitated with anti-IRS1 and proteins were separated by SDS/PAGE and characterized by anti-phosphotyrosine immunoblotting. Figure 6 shows that the phosphorylation of IRS1 due to the

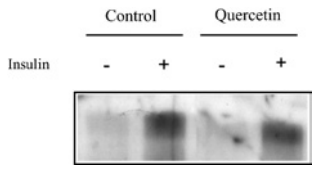

Figure 6 Lack of effect of quercetin on insulin-dependent IRS1 tyrosine phosphorylation in isolated adipocytes

Rat adipocytes were incubated with 100 μM quercetin at 37 °C for 30 s in a mixture containing Krebs–Ringer-Hepes buffer (pH 7.4), containing 1 % BSA, in the absence or presence of 1 μM insulin for 10 min. The cell suspension was immunoprecipitated with an anti-IRS1 antibody and then subjected to SDS/PAGE and Western blotting with an anti-phosphotyrosine antibody, as described in the Experimental section.

insulin treatment did not change with the presence of quercetin. Treatment with myricetin and catechin-gallate also showed the same effect as quercetin (results not shown). Therefore the inhibitory effects of myricetin, quercetin and catechin-gallate on the transport of glucose in adipocytes is apparently independent of phosphorylation–dephosphorylation reactions affecting IRS1.

GLUT4 3D molecular modelling

The GLUT4 model we propose adopts a right-handed α-helix barrel (Figure 7A), having 12-transmembrane α-helix segments surrounding a central pore. The N- and C-termini were modelled as random coil since good sequence templates are not available. Segments 2, 5, 7, 10 and 11 contain the most exposed residues from the internal pore view (Figure 7B).

The quality of the GLUT4 structure was reviewed with PROCHECK and Profiles-3D programs. For comparison, Table 1 shows the Ψ and Φ angles fulfilment, in a PROCHECK Ramachandran plot, for our GLUT4 model in comparison with GLUT3 and GLUT1 3D models [23,29], including crystallographic structures of the MscI [24], KcsA K^+ channel [30] and the AQP1 (aquaporin 1) water channel [31]. As can be seen from the GLUT4 Ramachandran plot, this model is at least as good as those for other proteins. GLUT4 has 2.8 % amino acids in disallowed regions, but none of them were involved in substrate docking. Our GLUT4 3D model shows the same proportion of Ψ and Φ misplaced angles as the template structure GLUT3 (Table 1). Furthermore, even though our structure has 2.8 % of disallowed residues, none of them belong to the QLS or ATP-binding domains, where our computer simulations were performed. In addition, the Profiles-3D analysis gives some regions misfolded for GLUT4 protein, but they are similar to those found in the reference structures GLUT3 and MscI (results not shown).

Table 1 PROCHECK Ramachandran scores for the structures of GLUT4, GLUT3, GLUT1, KcsA K^+ channel, AQP1 water channel and a gated mechanosensitive channel, MscI

	Favoured regions	Allowed regions	Generously allowed regions	Disallowed regions
GLUT4	73.3	21.5	2.4	2.8
GLUT3	77.2	18.2	1.7	2.9
GLUT1*	81.5	16.9	1.7	0
MscI†	74.5	23.4	2.1	0
KcsA‡	74.7	24.1	1.2	0
AQP1§	70.7	20.9	8.4	0

* PDB code 1JA5.
† PDB code 1MSL.
‡ PDB code 1BL8.
§ PDB code 1IH5.

Molecular dynamics simulated annealing

GLUT4 transporter has several residues related to D-glucose movement across the internal pore: Gln-295, Leu-296, Ser-297, Gln-298, Gln-299, Leu-300 and Ser-301, which constitute a motif known as 'QLS site' (Figure 7). To verify the accuracy

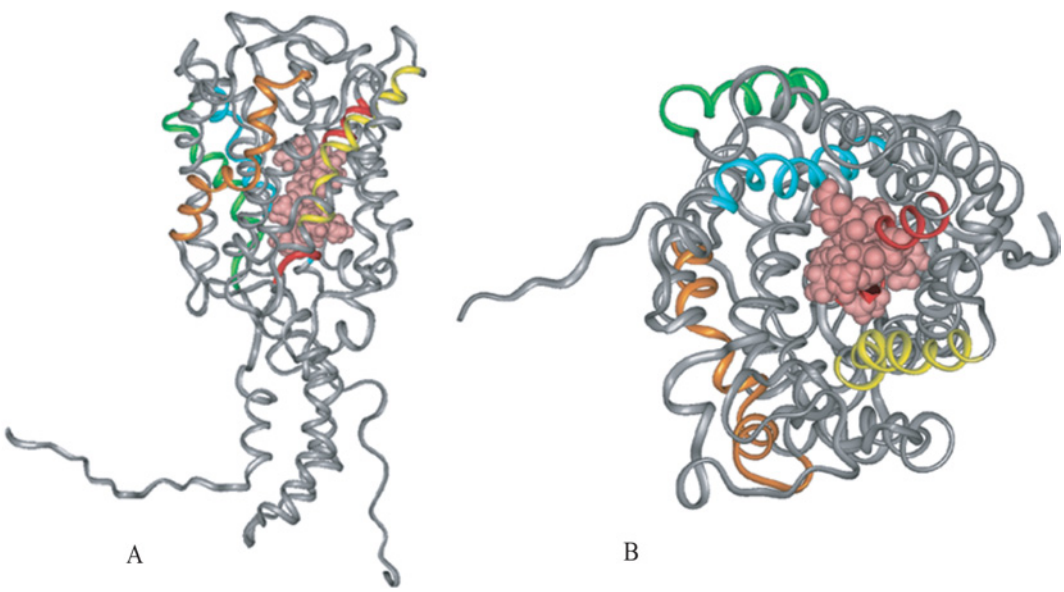

Figure 7 GLUT4 3D structure

(**A**) Ribbon representation (side view) of GLUT4 3D structure, showing the QLS site (pink) in CPK arrangement. C- and N-terminal regions are shown as a coil due to lack of a suitable template. (**B**) Extracellular top view in ribbon representation of GLUT4 3D structure. The QLS site, at the pore region in CPK arrangement (pink), comprises residues involved in glucose transport. Transmembrane helices are coloured: helix 2 (orange), helix 5 (yellow), helix 7 (red), helix 10 (green) and helix 11 (cyan).

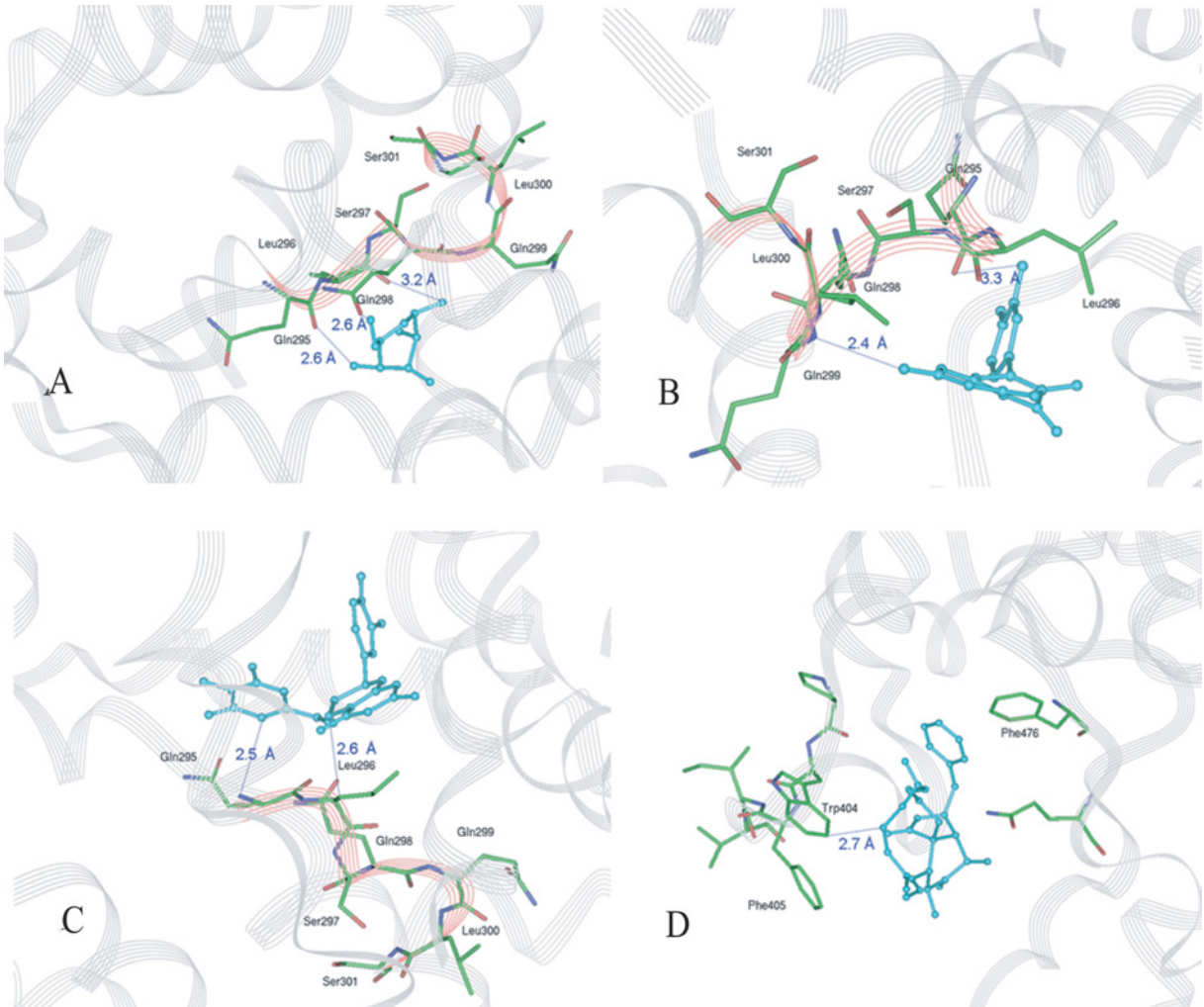

Figure 8 Computed structures for minimum energetic interactions from simulated annealing molecular dynamics docking procedures

Ligands appear in ball and stick arrangement, cyan-coloured. The GLUT4 structure appears as a grey transparent flat ribbon arrangement. The QLS motif is shown in red transparent flat ribbon arrangement and per atom coloured stick. (**A**) D-Glucose interaction with the QLS site. The distances between D-glucose and Gln-295 and between D-glucose and Leu-296 are 2.6 Å, whereas for Gln-298 the distance is 3.2 Å. Gln-295 and Leu-296 could form hydrogen bonds with glucose because of their proximity. (**B**) Quercetin interaction with the QLS site. The distance between quercetin and Gln-299 is 2.4 Å and, for Gln-298, it is 3.3 Å. Gln-299 could form a hydrogen bond with quercetin because of their proximity. (**C**) Interaction of catechin-gallate with the QLS site. The distance between catechin-gallate and Gln-295 is 2.5 Å and it is 2.6 Å for Leu-296. Catechin-gallate and Gln-295 could form a hydrogen bond and an aliphatic interaction could exist between the aromatic ring of catechin-gallate and the close aliphatic chain of Leu-296. (**D**) Interaction of cytochalasin B with the Trp-404 region, in a 10 Å interface for binding site definition. The distance between cytochalasin B and Trp-404 is 2.7 Å.

of the internal co-ordinates for our transporter, we proceeded to perform a docking procedure for D-glucose. At the simulation, D-glucose was found to interact directly (Figure 8A) through a non-bonded interaction with the QLS site. This evidence favours our transporter internal co-ordinates, giving a broad idea of what kind of interactions are responsible for ligand docking and transport.

Previous reports [32,33] have shown that cytochalasin B binds to the transmembrane domain of the glucose transporter in the vicinity of helices 10–11, either to Trp-388 or to Trp-412, as has been suggested by site-directed mutagenesis. Taking into account the amino acid sequence alignment and the conserved regions of the transporter isoforms, Trp-388 and Trp-412 in GLUT1 are equivalent to Trp-404 and Trp-428 in GLUT4. Our simulation data show the same kind of non-bonded interaction, having the most favourable energetic docking position when cytochalasin B interacts with Trp-404 (Figure 8D). When this molecule reaches its less energetic position, the transport of glucose through GLUT4 is blocked.

Docking simulations performed with the flavonoids quercetin and catechin-gallate revealed the same kind of interaction as that found for glucose with the QLS site when the docking position for every molecule reached the energetic minima (Figures 8B and 8C). Neither catechin nor gallic acid, simulated under the same conditions, reached a favourable energetic minimum (results not shown).

DISCUSSION

The flavonoids constitute a family of compounds with various biological effects [34]. In a previous report, we characterized the isoflavone genistein as a natural inhibitor of hexose and dehydroascorbic acid transport; genistein acts as a competitive inhibitor of the glucose transporter GLUT1 in HL-60 cells, Chinese-hamster ovary cells and human erythrocytes [9]. Later, it was shown in a systematic study that flavonoids, aglycones in particular, inhibit glucose uptake in U937 cells and Jurkat cells and that some structural characteristics correlate with this biological activity [8].

Additionally, it was found that flavonoids inhibit the intracellular accumulation of ascorbic acid; a specific role for GLUT1 and GLUT3 in dehydroascorbic acid uptake was proposed, and quercetin and myricetin were found to inhibit competitively the uptake of dehydroascorbic acid [7].

Our present results in adipocytes show that the flavonoids catechin-gallate, quercetin and myricetin inhibit the uptake of methylglucose (a substrate that enters the cells through the facilitative hexose transporter GLUT4) in insulin-stimulated rat adipocytes. In contrast, catechin and gallic acid added separately did not affect the activity of the transporter in adipocytes.

Insulin stimulates glucose transport in adipocytes through a mechanism involving the translocation of GLUT4, in which tyrosine phosphorylation plays a key role in the signal-transduction cascade [35]. Genistein, quercetin, apigenin and kaempferol have been described as tyrosine kinase inhibitors over the concentration range of 0.7–100 μg/ml [13]. Also, the direct interaction of GLUT1 at its nucleotide-binding motifs with a group of flavonoids that are tyrosine kinase inhibitors, flavones, isoflavones and related synthetic compounds, causes the inhibition of glucose and dehydroascorbic acid transport in a dose-dependent manner [10]. Our observation that quercetin, as well as myricetin and catechin-gallate (results not shown), had no significant effect on the phosphorylation of IRS1 in adipocytes, plus the lack of inhibition of tyrosine phosphorylation noted for heavily phosphorylated proteins of 185, 95 and 60 kDa (results not shown), support the hypothesis that the action of these compounds on glucose transport is due to a direct interaction with GLUT4.

A preincubation step was not necessary to observe the inhibitory effect of flavonoids on the uptake of methylglucose. The effect was instantaneous and maximal when the addition of flavonoid to the uptake assay medium was made simultaneously with the test substrate, at zero time. This instantaneous effect is different from that mediated by tyrosine kinase inhibition, a time-dependent phenomenon that usually requires a preincubation step with the inhibitor for full development [13,35,36].

Our docking data agree with previous findings for GLUT1, where D-glucose binds with the QLS site in the transport process [15,16]. Also, our data possibly explain the finding that epicatechin 3-gallate inhibits glucose exit from erythrocytes [37]. The computer simulations performed with D-glucose constitute a positive control for the model co-ordinates at the QLS site.

Analysis of our docking data and the experimental results obtained for quercetin and catechin-gallate support the conclusion that flavonoids are competitive blockers of glucose transport, through a direct interaction with the QLS site. Both molecules interact directly, in their most favourable energetic position, with the residues arranged in the QLS site. The use of a spherical interface with a 20 Å radius around Gln-295, in which every residue was defined as mobile and part of the active site, ensured that not only Gln-295 could be involved in the most favourable energetic position finding, but also any other residue contained within the 20 Å-radius sphere. Residues located at α-helices 2, 5, 7, 10 and 11 are inside this sphere. As a control for this simulation, catechin and gallic acid by themselves, and in contrast with catechin-gallate, were not able to find favourable energetic positions at their interaction with the QLS site.

In summary, the present study has shown that quercetin, myricetin and catechin-gallate inhibit the transport of glucose in isolated rat adipocytes stimulated with insulin in the concentration range 20–100 μM and that, apparently, these flavonoids do not inhibit glucose transport by inhibiting the tyrosine kinase activity acting on IRS1. These data are consistent with the evidence presented, indicating a direct interaction of flavonoids with GLUT4. The fact that computer simulation suggests that the interaction of flavonoids with GLUT4 occurs at the same residues as glucose, in the pore region, and the glucose transport inhibition studies in adipocytes reported, constitute strong evidence in support of the hypothesis that GLUT4, and perhaps GLUTs in general, play an important role in flavonoid uptake. Maybe the tissue specificity and transport selectivity of the different GLUTs will help in understanding the various biological effects of these natural polyphenols.

This work was supported by PUC-PBMEC (Pontificia Universidad Catolica de Chile – Programa Bases Moleculares de las Enfermedades Cronicas) 2000–2003 programme.

REFERENCES

1 Simpson, I. A. and Cushman, S. W. (1986) Hormonal regulation of mammalian glucose transport. Annu. Rev. Biochem. **55**, 1059–1089

2 Czech, M. P. and Corvera, S. (1999) Signaling mechanisms that regulate glucose transport. J. Biol. Chem. **274**, 1865–1868

3 Zorzano, A., Wilkinson, W., Kotliar, N., Thoidis, G., Wadzinkski, B. E., Ruoho, A. E. and Pilch, P. F. (1989) Insulin-regulated glucose uptake in rat adipocytes is mediated by two transporter isoforms present in at least two vesicle populations. J. Biol. Chem. **264**, 12358–12363

4 Cushman, S. W. and Wardzala, L. J. (1980) Potential mechanism of insulin action on glucose transport in the isolated rat adipose cell. Apparent translocation of intracellular transport systems to the plasma membrane. J. Biol. Chem. **255**, 4758–4762

5 Macheix, J. J., Fleuriet, A. and Billot, J. (1990) The Fruit Phenolics, CRC Press, Boca Raton, FL

6 Hertog, M. G., Hollman, P. C., Katan, M. B. and Kromhout, D. (1993) Intake of potentially anticarcinogenic flavonoids and their determinants in adults in the Netherlands. Nutr. Cancer **20**, 21–29

7 Park, J. B. and Levine, M. (2000) Intracellular accumulation of ascorbic acid is inhibited by flavonoids via blocking of dehydroascorbic acid and ascorbic acid uptakes in HL-60, U937 and Jurkat cells. J. Nutr. **130**, 1297–1302

8 Park, J. B. (1999) Flavonoids are potential inhibitors of glucose uptake in U937 cells. Biochem. Biophys. Res. Commun. **260**, 568–574

9 Vera, J. C., Reyes, A. M., Carcamo, J. G., Velasquez, F. V., Rivas, C. I., Zhang, R. H., Strobel, P., Iribarren, R., Scher, H. I., Slebe, J. C. et al. (1996) Genistein is a natural inhibitor of hexose and dehydroascorbic acid transport through the glucose transporter, GLUT1. J. Biol. Chem. **271**, 8719–8724

10 Vera, J. C., Reyes, A. M., Velasquez, F. V., Rivas, C. I., Zhang, R. H., Strobel, P., Slebe, J. C., Nunez-Alarcon, J. and Golde, D. W. (2001) Direct inhibition of the hexose transporter GLUT1 by tyrosine kinase inhibitors. Biochemistry **40**, 777–790

11 Spencer, J. P., Abd-el-Mohsen, M. M. and Rice-Evans, C. (2004) Cellular uptake and metabolism of flavonoids and their metabolites: implications for their bioactivity. Arch. Biochem. Biophys. **423**, 148–161

12 Walle, T. (2004) Absorption and metabolism of flavonoids. Free Radical Biol. Med. **36**, 829–837

13 Akiyama, T., Ishida, J., Nakagawa, S., Ogawara, H., Watanabe, S., Itoh, N., Shibuya, M. and Fukami, Y. (1987) Genistein, a specific inhibitor of tyrosine-specific protein kinases. J. Biol. Chem. **262**, 5592–5595

14 Smith, R. M., Tiesinga, J. J., Shah, N., Smith, J. A. and Jarett, L. (1993) Genistein inhibits insulin-stimulated glucose transport and decreases immunocytochemical labeling of GLUT4 carboxyl-terminus without affecting translocation of GLUT4 in isolated rat adipocytes: additional evidence of GLUT4 activation by insulin. Arch. Biochem. Biophys. **300**, 238–246

15 Hruz, P. W. and Mueckler, M. M. (2001) Structural analysis of the GLUT1 facilitative glucose transporter. Mol. Membr. Biol. **18**, 183–193

16 Carruthers, A. (1990) Facilitated diffusion of glucose. Physiol. Rev. **70**, 1135–1176

17 Alvarez, J., Lee, D. C., Baldwin, S. A. and Chapman, D. (1987) Fourier transform infrared spectroscopic study of the structure and conformational changes of the human erythrocyte glucose transporter. J. Biol. Chem. **262**, 3502–3509

18 Cloherty, E. K., Hamill, S., Levine, K. and Carruthers, A. (2001) Sugar transporter regulation by ATP and quaternary structure. Blood Cells Mol. Dis. **27**, 102–107

19 Rodbell, M. (1964) Metabolism of isolated fat cells. I. Effects of hormones on glucose metabolism and lipolysis. J. Biol. Chem. **239**, 375–380

20 Whitesell, R. R. and Gliemann, J. (1979) Kinetic parameters of transport of 3-O-methylglucose and glucose in adipocytes. J. Biol. Chem. **254**, 5276–5283

21 Walgren, R. A., Lin, J. T., Kinne, R. K. and Walle, T. (2000) Cellular uptake of dietary flavonoid quercetin 4′-beta-glucoside by sodium-dependent glucose transporter SGLT1. J. Pharmacol. Exp. Ther. **294**, 837–843

22 Laemmli, U. K. (1970) Cleavage of structural proteins during the assembly of the head of bacteriophage T4. Nature (London) **227**, 680–685
23 Dwyer, D. S. (2001) Model of the 3-D structure of the GLUT3 glucose transporter and molecular dynamics simulation of glucose transport. Proteins **42**, 531–541
24 Chang, G., Spencer, R. H., Lee, A. T., Barclay, M. T. and Rees, D. C. (1998) Structure of the MscL homolog from *Mycobacterium tuberculosis*: a gated mechanosensitive ion channel. Science **282**, 2220–2226
25 Laskowski, R. A., MacArthur, M. W., Moss, D. S. and Thornton, J. M. (1993) PROCHECK: a program to check the stereochemical quality of protein structures. J. Appl. Cryst. **26**, 283–291
26 Afzal, I., Cunningham, P. and Naftalin, R. J. (2002) Interactions of ATP, oestradiol, genistein and the anti-oestrogens, faslodex (ICI 182780) and tamoxifen, with the human erythrocyte glucose transporter, GLUT1. Biochem. J. **365**, 707–719
27 White, M. F. and Kahn, C. R. (1994) The insulin signaling system. J. Biol. Chem. **269**, 1–4
28 Shisheva, A. and Shechter, Y. (1992) Quercetin selectively inhibits insulin receptor function *in vitro* and the bioresponses of insulin and insulinomimetic agents in rat adipocytes. Biochemistry **31**, 8059–8063
29 Zuniga, F. A., Shi, G., Haller, J. F., Rubashkin, A., Flynn, D. R., Iserovich, P. and Fischbarg, J. (2001) A three-dimensional model of the human facilitative glucose transporter Glut1. J. Biol. Chem. **276**, 44970–44975
30 Doyle, D. A., Morais Cabral, J., Pfuetzner, R. A., Kuo, A., Gulbis, J. M., Cohen, S. L., Chait, B. T. and MacKinnon, R. (1998) The structure of the potassium channel: molecular basis of K^+ conduction and selectivity. Science **280**, 69–77
31 Ren, G., Reddy, V. S., Cheng, A., Melnyk, P. and Mitra, A. K. (2001) Visualization of a water-selective pore by electron crystallography in vitreous ice. Proc. Natl. Acad. Sci. U.S.A. **98**, 1398–1403
32 Inukai, K., Asano, T., Katagiri, H., Anai, M., Funaki, M., Ishihara, H., Tsukuda, K., Kikuchi, M., Yazaki, Y. and Oka, Y. (1994) Replacement of both tryptophan residues at 388 and 412 completely abolished cytochalasin B photolabelling of the GLUT1 glucose transporter. Biochem. J. **302**, 355–361
33 Garcia, J. C., Strube, M., Leingang, K., Keller, K. and Mueckler, M. M. (1992) Amino acid substitutions at tryptophan 388 and tryptophan 412 of the HepG2 (Glut1) glucose transporter inhibit transport activity and targeting to the plasma membrane in Xenopus oocytes. J. Biol. Chem. **267**, 7770–7776
34 Rice-Evans, C. and Packer, L. (1998) Flavonoids in Health and Disease (Rice-Evans, C. A. and Packer, L., eds.), Marcel Dekker, Inc., New York, Basel
35 Watanabe, T., Kondo, K. and Oishi, M. (1991) Induction of *in vitro* differentiation of mouse erythroleukemia cells by genistein, an inhibitor of tyrosine protein kinases. Cancer Res. **51**, 764–768
36 Linassier, C., Pierre, M., Le Pecq, J. B. and Pierre, J. (1990) Mechanisms of action in NIH-3T3 cells of genistein, an inhibitor of EGF receptor tyrosine kinase activity. Biochem. Pharmacol. **39**, 187–193
37 Naftalin, R. J., Afzal, I., Cunningham, P., Halai, M., Ross, C., Salleh, N. and Milligan, S. R. (2003) Interactions of androgens, green tea catechins and the antiandrogen flutamide with the external glucose-binding site of the human erythrocyte glucose transporter GLUT1. Br. J. Pharmacol. **140**, 487–499

Received 29 April 2004/27 September 2004; accepted 7 October 2004
Published as BJ Immediate Publication 7 October 2004, DOI 10.1042/BJ20040703